

Theoretical study on the Rydberg states of NeH: *Ab initio* quantum defect and complex coordinate calculations

Ioannis D. Petsalakis and Giannoula Theodorakopoulos

*Theoretical and Physical Chemistry Institute, The National Hellenic Research Foundation,
48 Vas. Constantinou Ave., Athens 116 35, Greece*

Yan Li, Gerhard Hirsch, and Robert J. Buenker

*Fachbereich 9- Theoretische Chemie, Bergische Universität-Gesamthochschule Wuppertal,
Gaussstr. 20, D-42097 Wuppertal, Germany*

Mark S. Child

*Physical and Theoretical Chemistry Laboratory, Oxford University, South Parks Road,
Oxford OX1 3QZ, United Kingdom*

(Received 23 October 1997; accepted 6 February 1998)

Ab initio calculations have been carried out on the potential energy curves of the Rydberg states of NeH up to $3d$. Quantum defect functions have been calculated from the *ab initio* potentials and potential energy curves and vibrational levels for higher n (s, p, d) Rydberg states have been generated. The interaction of the $2p$ $B^2\Pi$ state with the $2s$ and $2p$, $A^2\Sigma^+$ and $C^2\Sigma^+$ states and their predissociation by $X^2\Sigma^+$ has been treated by multi-state complex coordinate scaling calculations for both NeH and NeD. The results are consistent with previous 2×2 calculations on the predissociation of the $A^2\Sigma^+$ and $C^2\Sigma^+$ states. Finally, a calculation of the interaction between the 2Π , $2\Sigma^+$, and 2Δ $3d$ states in NeH and NeD shows appreciable mixing between the states at high values of the rotational quantum number. © 1998 American Institute of Physics. [S0021-9606(98)02518-5]

I. INTRODUCTION

There is continuing interest in the Rydberg spectra of diatomic rare-gas hydrides, also called Rydberg molecules.¹ With a single electron outside a stable closed shell core, these systems have repulsive ground electronic states with only shallow van der Waals minima and stacks of bound Rydberg states.² The first such spectra were observed in 1970 by Johns for ArH and ArD.³ In 1985 a spectrum of bound HeH was reported⁴ and following that a great deal of experimental work on the Rydberg spectra of the rare gas-hydrides has appeared. Bound-bound as well as bound-repulsive spectra have been obtained for all RgH systems (with Rg=He, Ne, Ar, Kr and Xe) and detailed analyses of Rydberg spectra of HeH (Ref. 5) and also of the larger systems, ArH, KrH and XeH (Ref. 6, and references therein) have been reported. The situation regarding NeH is different. Bound-repulsive spectra of NeH were observed in 1987 (Ref. 7) and there have been some further studies of the dissociative decay of excited states of NeH and NeD.⁸⁻¹⁰ However, bound-bound spectra of NeH have not been analyzed, although some bands have been observed and reported in 1986 and 1988,^{11,12} where however, the low intensity of the spectra did not allow their further analysis. Since then there have been no other reports of discrete spectra of NeH, despite all the activity regarding the rare gas hydrides. In terms of theoretical calculations, the electronic states of NeH have been treated in an early study,² along with HeH and ArH and in subsequent work,¹³⁻¹⁶ providing information on the potential energy curves of the lower lying states (up to $3p$), vertical

energies and radiative lifetimes (for states up to $3d$) and predissociation lifetimes of the $A^2\Sigma^+$ and $C^2\Sigma^+$ states in NeH and the $A^2\Sigma^+$ state in NeD. In general, it appears that predissociation is not as important in NeH and NeD as it is in the He and Ar analogs^{14,15} where the $A^2\Sigma^+$ states have lifetimes of only a few ps. Secondly, it was found that predissociation of the $A^2\Sigma^+$ state in NeD was strongly suppressed, compared to NeH, and this result, which is consistent with experimental observations,⁸ has been explained in terms of overlap integrals and expectation values of the derivatives of the vibrational functions with respect to the internuclear distance R .^{8,17}

In the present work, a further theoretical effort on the structure of NeH is reported, which might aid future experimental studies on the Rydberg spectra of this system. In particular, *ab initio* potential energy curves which have been calculated for the Rydberg states up to $3d$ and the ground state of the cation, NeH^+ , have been employed for the calculation of quantum defect functions which may in turn be employed for the generation of the potential energy curves and vibrational levels of all the higher n , s , p and d Rydberg states. Secondly, the predissociation of the $2s$ and $2p$ ($A^2\Sigma^+$, $C^2\Sigma^+$, and $B^2\Pi$) states is investigated by a recently developed multi-state complex scaling procedure,^{18,19} where the interactions between the $X^2\Sigma^+$, $A^2\Sigma^+$, $C^2\Sigma^+$, and $B^2\Pi$ states are taken into account simultaneously. In the analyses of the observed spectra in ArH the lowest p states are treated as a “ p complex,”²⁰ which in the *ab initio* calculations was manifested by the very small $2\Sigma^+ - 2\Pi$ en-

ergy splitting and the large interaction (rotational electronic coupling) between them.²¹ Thus the present multi-state calculations examine the extent of formation of such a complex in the $n=2$ Rydberg states of NeH and NeD and its effect on the rates of their predissociation by the repulsive ground state. Similarly, the formation of a $3d$ complex in NeH and in NeD is investigated in the present work by a multi-state vibrational calculation including the three $3d$ states ($D^2\Sigma^+$, $E^2\Pi$, and $1^2\Delta$) and their mutual interactions.

II. CALCULATIONS

A. *Ab initio* calculations

Ab initio MRDCI (Ref. 22) calculations have been carried out on 11 electronic states of NeH, six $^2\Sigma^+$, four $^2\Pi$ and the first $^2\Delta$, in C_{2v} symmetry. Similarly, the ground state of NeH⁺, $^1\Sigma^+$, was calculated.

The atomic orbital (AO) basis set is similar to those employed in our previous work on the rare gas hydrides. For hydrogen the $(6s/4s)$ basis set of Huzinaga²³ was augmented with one p polarization function and Rydberg s , p and d functions²¹ while for Ne the $(11s6p/5s4p)$ basis set²⁴ was augmented with diffuse s and p functions and 2 d polarization functions.²⁵ The configuration interaction (CI) spaces were generated by all single and double excitations with respect to reference spaces consisting of 22 configurations for the 2A_1 ($^2\Sigma^+$ and $^2\Delta$) states, 13 configurations for the 2B_1 ($^2\Pi$) states and 43 configurations for the ionic states. Selection of configurations for the actual diagonalization with respect to 7, 4 and 2 roots respectively and energy threshold of 2.5 microhartree was carried out. Extrapolation to zero threshold and full-CI correction²⁶ was applied to the eigenvalues.

The MRDCI calculations were carried out for different values of the internuclear distance R , varying from 1.2 bohr to 100.0 bohr. At each value of R , along with the energy, the rotational-electronic coupling between the 2A_1 and the 2B_1 states has been also calculated. Thus the computed matrix elements need to be multiplied by $\sqrt{2}$ for the corresponding Σ - Π and by 2 for the Π - Δ interactions.

B. Quantum defect calculations

The potential energy curves $V_{inl\lambda}(R)$ of the $l\lambda$ Rydberg states converging on the positive ion potential $V_i^+(R)$ are related to the quantum defect function $\mu_{il\lambda}(R)$,

$$V_{inl\lambda}(R) = V_i^+(R) - \frac{R_y}{(n - \mu_{il\lambda}(R))^2}, \quad (1)$$

where R_y is the Rydberg constant and R is the internuclear distance.

Equation (1) is used below to determine the quantum defect functions from the *ab initio* potentials. The label $l\lambda$ is symbolic because the Born-Oppenheimer quantum defects belong to l -mixed states. Such l -mixing is represented by off-diagonal quantum defects in a full multichannel quantum defect calculation.²⁷⁻³³ In the present work single-channel quantum defect analysis is carried out for the generation of the potential energy curves and vibrational levels of all the higher n Rydberg states of NeH.

Instead of the quantum defects $\mu_{il\lambda}(R)$ of Eq. (1), it is more convenient to work with $\eta_{il\lambda}(R)$ which are determined by

$$\tan \pi \eta_i(R) + \frac{\tan \pi \nu_i(R)}{A_{l_i}(\nu_i(R))} = 0, \quad (2)$$

where

$$\nu_i(R) = [2(V_i^+(R) - E(R))]^{-1/2}, \quad (3)$$

$$A_{l_i}(\nu_i(R)) = \prod_{k=0}^{l_i} \left(1 - \frac{k^2}{\nu_i^2} \right), \quad (4)$$

and $E(R)$ represents the energies of the Rydberg states. The factor $[A_{l_i}(\nu_i(R))]^{-1}$ serves to eliminate solutions with $l_i < n_i$.²⁷

Equation (2) is employed first, with the *ab initio* potentials substituted for $E(R)$, for the determination of the quantum defects. The higher Rydberg states are calculated subsequently by introducing the calculated quantum defect functions in Eq. (2) and varying $E(R)$ to find those energies which satisfy the equation.

In general, there is some energy dependence in the quantum defects calculated as above and this may be incorporated in the $\eta_{il\lambda}(R)$ functions and the subsequent calculation of higher Rydberg states.

The quantum defect functions may be used to calculate the vibrational levels of different electronic states.³¹ A vibrational K matrix is constructed,

$$K_{\nu_+ \nu'_+} = \langle \nu_+ | A_{l_i}[\nu(R)] \tan \pi \eta_{il\lambda}(R) | \nu'_+ \rangle, \quad (5)$$

where $|\nu_+\rangle$ are vibrational functions of the positive ion. The vibrational levels of the Rydberg states are obtained by finding the energy levels E for which

$$\det(K_{\nu_+ \nu'_+} + \tan \pi \nu_{\nu_+}(E)) = 0, \quad (6)$$

where $\tan \pi \nu_{\nu_+}(E)$ is a diagonal matrix such that

$$\nu_{\nu_+}(E) = [2(E_{\nu_+} - E)]^{-1/2}. \quad (7)$$

C. Multi-state vibrational calculations involving complex scaling of the internuclear coordinate

The transformation of the nuclear coordinate $R \rightarrow \rho = Re^{i\theta}$ with θ real, allows the calculation of energies and widths of predissociation resonances in terms of square integrable functions by solution of a complex eigenvalue problem

$$|H - z| = 0, \quad (8)$$

where z is the diagonal matrix of complex eigenvalues.³⁴⁻³⁶ The resonances correspond to the eigenvalues z_k which are stable with respect to θ and

$$z_k = E_k - \frac{i}{2} \Gamma_k \quad (9)$$

with E_k the energy position and Γ_k the linewidth of the resonance.

The particular implementation of the theory in the present work involves simultaneous treatment of a number of

interacting electronic states, namely the $X^2\Sigma^+$, $A^2\Sigma^+$, $B^2\Pi$ and $C^2\Sigma^+$ states of NeH and NeD. The *ab initio* adiabatic potentials and the rotational-electronic coupling matrix elements (for $^2\Sigma^+ - ^2\Pi$ interactions) calculated in the present work along with the radial coupling matrix elements (for $^2\Sigma^+ - ^2\Sigma^+$ interactions) of previous work¹³ are employed in the present calculation.

The Hamiltonian matrix in Eq. (8) consists of blocks H^{IJ} where I, J stand for the different electronic states. A basis set of Hermite polynomials is employed,

$$y_n(R) = \left[\left(\frac{a}{\pi} \right)^{1/4} \frac{1}{\sqrt{2^n n!}} \right] e^{(-aR^2/2)} H_n(\sqrt{a}R), \quad (10)$$

and matrix elements over the nuclear energy operator and over the electronic potential energy functions and interactions are computed. In the evaluation of these matrix elements use is made of the back-rotation identity, which holds for square-integrable functions³⁷

$$\langle \psi_i(R) | H(\rho) | \psi_j(R) \rangle = \langle \psi_i(\rho^*) | H(R) | \psi_j(\rho^*) \rangle, \quad (11)$$

where ρ^* is the complex conjugate of ρ , corresponding to a complex rotation of R by $-\theta$. In this manner, it is not required to perform a complex rotation on the potentials but only on the basis functions.

The matrix elements of the nuclear kinetic energy operator over the (complex-rotated) basis functions y_n of Eq. (3) can be evaluated analytically,

$$\begin{aligned} T_{nm} &= \frac{e^{-2i\theta} a}{2\mu} \left(n + \frac{1}{2} \right) \quad \text{for } n=m \\ T_{nm} &= -\frac{e^{-2i\theta} a}{2\mu} \frac{\sqrt{(n+1)(n+2)}}{2} \quad \text{for } n=m+2 \\ T_{nm} &= 0 \quad \text{otherwise.} \end{aligned} \quad (12)$$

The matrix elements over the electronic potentials are given by

$$\begin{aligned} V_{nm} &= \left(\frac{a}{\pi} \right)^{1/2} \frac{e^{-i\theta}}{2^{n/2}(n!)^{1/2}} \frac{1}{2^{m/2}(m!)^{1/2}} \int e^{-ae^{-2i\theta}R^2} \\ &\quad \times H_n(\sqrt{a}Re^{-i\theta}) V(R) H_m(\sqrt{a}Re^{-i\theta}) dR, \end{aligned} \quad (13)$$

where $V(R)$ stands for an adiabatic electronic potential energy curve. The matrix elements (13) are evaluated numerically with the aid of a Gauss-Hermite quadrature procedure, following one further coordinate transformation, $y = R\sqrt{a} \cos(2\theta)$. Spline interpolation between the *ab initio* energies is employed to generate additional points as required by the numerical procedure. Finally, it is convenient to avoid explicit computation of the factorials by defining functions

$$C_n(R) = \frac{H_n(R)}{2^{n/2}(n!)^{1/2}} \quad (14)$$

with the recurrence relations

$$\begin{aligned} C_0(R) &= 1, \quad C_1(R) = \sqrt{2}R, \\ C_n &= \sqrt{\frac{2}{n}} C_{n-1} - \sqrt{\frac{n-1}{n}} C_{n-2}. \end{aligned} \quad (15)$$

In terms of these functions (14), the matrix elements (13) become,

$$\begin{aligned} V_{nm} &= \frac{e^{-i\theta}}{\sqrt{\pi} \cos 2\theta} \int e^{-y^2} e^{i \tan 2\theta y^2} \\ &\quad \times C_n \left(\frac{ye^{-i\theta}}{\sqrt{\cos 2\theta}} \right) V \left(\frac{y}{\sqrt{a} \cos 2\theta} \right) C_m \left(\frac{ye^{-i\theta}}{\sqrt{\cos 2\theta}} \right) dy. \end{aligned} \quad (16)$$

Analogous expressions are obtained for the interaction matrix elements when the interaction involves rotational-electronic coupling. In this case, $V(R)$ of Eq. (13) stands for $-(1/2\mu)\sqrt{N' \pm \Lambda'}(N' + 1 \mp \Lambda')$ $\langle \psi_l | (L_{\pm}/R^2) | \psi_j \rangle$. For radial coupling, the matrix element over the first derivative with respect to the internuclear distance, $(-1/\mu)A(R)\partial/\partial R$, becomes

$$\begin{aligned} V_{nm} &= -\frac{\sqrt{\alpha}e^{-2i\theta}}{\mu\sqrt{\pi} \cos 2\theta} \int e^{-y^2} e^{i \tan 2\theta y^2} C_n \left(\frac{ye^{-i\theta}}{\sqrt{\cos 2\theta}} \right) \\ &\quad \times A \left(\frac{y}{\sqrt{a} \cos 2\theta} \right) \times \left[2m C_{m-1} \left(\frac{ye^{-i\theta}}{\sqrt{\cos 2\theta}} \right) - \sqrt{\alpha}e^{-i\theta} \right. \\ &\quad \left. \times \frac{y}{\sqrt{a} \cos 2\theta} C_m \left(\frac{ye^{-i\theta}}{\sqrt{\cos 2\theta}} \right) \right] dy, \end{aligned} \quad (17)$$

while for the second derivative interaction, $-(1/2\mu)B(R)$, the matrix elements are analogous to those in Eq. (13). In the above, $A(R)$ and $B(R)$ stand for the matrix elements of the first and the second derivatives of the electronic wavefunctions evaluated at different values of R .

Once the required matrix elements are evaluated Eq. (8) is set up and solved for a given basis set at different values of θ and the stable eigenvalues z_k correspond to the required resonances. Convergence with respect to the basis set size is sought. In the present calculations, different-sized basis sets have been employed, ranging from 90 to 300 functions per electronic state. It was found that convergence was reached with 120 functions per state, with stabilization for rotation angles θ up to 10° . The results presented in the next section have been obtained with a basis set of 200 functions.

The predissociation lifetime τ in seconds is obtained from the linewidth Γ in atomic units,

TABLE I. Calculated energies (hartree)^a of electronic states of NeH and the ground state of NeH⁺.

$R(a.u.)$	$X^2\Sigma^+$	$A^2\Sigma^+(2s)$	$C^2\Sigma^+(2p)$	$D^2\Sigma^+(3d)$	$5^2\Sigma^+(3s)$	$6^2\Sigma^+(3p)$	$1^2\Delta(3d)$	$B^2\Pi(2p)$	$E^2\Pi(3p)$	$3^2\Pi(3p)$	$X^1\Sigma^+$
1.2	.43766	.52583	.56274	.58048	.58630	.59993	.58230	.52834	.57973	.58615	.63478
1.4	.28209	.38262	.41642	.43702	.44301	.45544	.43926	.38626	.43762	.44404	.49204
1.6	.20317	.32317	.35397	.37992	.38567	.39633	.38258	.32868	.38024	.38652	.43493
1.8	.15163	.30273	.32930	.36109	.36649	.37562	.36432	.31006	.36177	.36813	.41645
2.0	.11319	.30082	.32477	.36083	.36581	.37391	.36443	.30984	.36202	.36813	.41616
2.2	.08419	.30853	.32980	.36938	.37428	.38154	.37293	.31682	.36961	.37557	.42387
2.4	.06179	.31776	.33766	.37915	.38364	.39062	.38301	.32691	.38041	.38604	.43450
2.6	.04521	.32893	.34789	.39092	.39535	.40198	.39421	.33655	.39139	.39662	.44564
2.8	.03241	.33992	.35911	.40328	.40704	.41374	.40618	.34591	.40171	.40671	.45591
3.0	.02326	.34834	.36705	.41145	.41492	.42167	.41425	.35387	.41086	.41550	.46477
3.5	.01021	.36248	.38208	.42721	.43684	.42974	.42974	.36591	.42677	.42993	.48064
4.0	.00435	.36886	.38913	.43608	.43710	.44412	.43732	.37198	.43582	.43814	.48897
4.5	.00165	.37247	.39158	.44061	.44139	.44789	.44159	.37437	.43992	.44159	.49325
5.0	.00071	.37333	.39008	.44262	.44329	.44867	.44341	.37513	.44191	.44310	.49510
6.0	.00023	.37497	.38575	.44406	.44520	.44920	.44489	.37545	.44378	.44449	.49719
7.0	.00013	.37500	.38110	.44430	.44504	.44883	.44501	.37550	.44440	.44511	.49809
8.0	.00002	.37509	.37837	.44433	.44482	.44923	.44518	.37521	.44441	.44495	.49831
9.0	.00052	.37562	.37732	.44495	.44543	.44972	.44582	.37512	.44491	.44502	.49831
10.0	.00084	.37592	.37679	.44530	.44582	.44974	.44614	.37530	.44498	.44514	.49862
20.0	.00027	.37521	.37577	.44475	.44557	.44575	.44561	.37514	.44495	.44513	.49870
100.0	.0	.37499	.37554	.44451	.44540	.44541	.44540	.37500	.44484	.44488	.49871

^aZero energy is -129.28347 hartree.

$$\tau = \frac{2.41888 \times 10^{-17}}{\Gamma} \quad (18)$$

III. RESULTS AND DISCUSSION

A. *Ab initio* calculations

The *ab initio* energies for the ground and Rydberg states of NeH and the ground state of NeH⁺ are listed in Table I. A plot of the calculated potential energy curves is given in Fig. 1. The present potential of NeH⁺ yields ω_e 2879 cm⁻¹, B_e 17.465 cm⁻¹, $\omega_e x_e$ 112.75 cm⁻¹, r_e 1.895 bohr, D_0 2.11 eV and D_e 2.29 eV. These values are very close to previous theoretical and experimental data.³⁸

The calculated energies for states of NeH (cf. Table I) are lower than those previously calculated but in terms of transition energies the results for the first three states are very close to the previous calculations,^{2,13} within 0.01 eV. At the dissociation limits, the transition energies correspond to atomic hydrogen excitation energies. The calculated energies at 100.0 bohr (cf. Table I) yield excitation energies only 105 ± 40 cm⁻¹ above the relevant H atom limits. Similarly the ionization energy at 100 bohr is 280 cm⁻¹ lower than the hydrogen atom ionization potential. It is not possible to make a corresponding comparison of the molecular excitation energies, in the absence of the appropriate experimental data. It is expected that the errors in the theoretical molecular transition energies shall not exceed the above discrepancies occurring in the atomic transition energies.

Tentative assignment of the observed bandheads in the Rydberg spectra of NeH at 6850, 7745 and 8490 Å¹² corresponding to 14599, 12912 and 11779 cm⁻¹ are suggested to calculated transitions $5^2\Sigma^+ - A^2\Sigma^+$ at 14265 cm⁻¹,

$D^2\Sigma^+ - A^2\Sigma^+$ at 13171 cm⁻¹ and $E^2\Pi - B^2\Pi$ at 11450 cm⁻¹ (where the given energy differences are obtained from the electronic energies at 2.0 bohr). Previous calculations¹³ have obtained radiative lifetimes of 22.0 ns and 20.8 ns for $D^2\Sigma^+$ and $E^2\Pi$ states, respectively. The

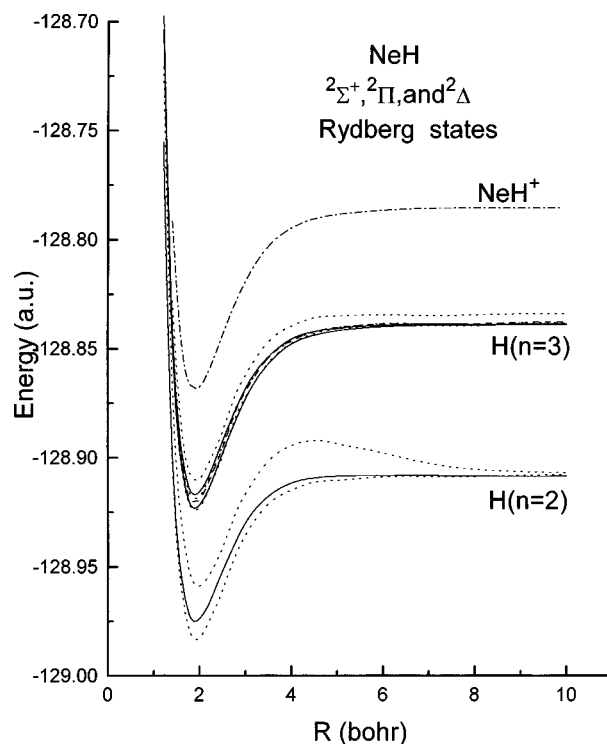


FIG. 1. *Ab initio* potential energy curves of Rydberg states of NeH and the ground electronic state of NeH⁺. Dotted lines $2^2\Sigma^+$ states, solid lines $2^2\Pi$ and dashed lines $2^2\Delta$ states.

TABLE II. Expansion coefficients of the quantum defect functions [cf. Eq. (19)].

Channel		a_0	a_1	a_2	a_3	a_4
$A\ 2\Sigma^+$	$2s$	-0.403671	0.360037	-0.144899	0.026389	-0.001740
$5\ 2\Sigma^+$	$3s$	-0.400431	0.331397	-0.153137	0.031371	-0.002257
$C\ 2\Sigma^+$	$2p$	-1.733537	1.464646	-0.543827	0.087492	-0.005024
$D\ 2\Sigma^+$	$3d$	-0.566438	0.876953	-0.429158	0.080233	-0.005134
$1\ 2\Delta$	$3d$	-0.045648	0.021993	-0.075263	0.023163	-0.001929
$B\ 2\Pi$	$2p$	0.001915	-0.299014	0.143160	-0.023678	0.001334
$3\ 2\Pi$	$3p$	0.033592	-0.340573	0.159178	-0.027231	0.001624
$E\ 2\Pi$	$3d$	0.132124	-0.153410	0.065186	-0.013974	0.001081

atomic labels of the states given in Table I, correspond to the predominant l character of the molecular states at 2.0 bohr. As mentioned previously the calculated adiabatic states are l -mixed and the character of the states varies with R . An estimate of the l -mixing may be obtained from the CI coefficients, when the SCF orbitals are not heavily mixed. Here, for R larger than 2.0 bohr this holds. Thus for $R=2.5$ bohr there are two important configurations for the $A\ 2\Sigma^+$ state, with c^2 of 0.896 (s configuration) and 0.051 (p configuration) while for $C\ 2\Sigma^+$ the corresponding c^2 are 0.054 (s) and 0.895 (p). At larger R there is less mixing. For example at $R=10$ bohr, the two states above are characterized by a single configuration each (s for $A\ 2\Sigma^+$ and p for $C\ 2\Sigma^+$) with c^2 of 0.971. At $R \leq 2.0$ bohr, the l -mixing occurs mostly at the SCF level. Since the SCF coefficients are over non-orthonormal basis functions, they cannot be used directly. One way to obtain an estimate of the l -mixing in this case would be to carry out a transformation of the adiabatic states into pure- l diabatic states. Such a transformation is beyond the scope of the present work.

B. Quantum defect calculations

The *ab initio* energies at different R have been employed for the calculation of quantum defects as described in the previous section. At this point the potential energy curve of the cation is shifted uniformly by 0.001 030 hartree in order to eliminate the error in the theoretical ionization potential.

The quantum defects obtained at different values of R , from 1.2 to 6.0 bohr, are expressed in terms of a polynomial of fourth order,

$$\eta_i(R) = \sum_{j=0}^4 a_j R^j. \quad (19)$$

The resulting expansion coefficients are given in Table II, while a plot of the corresponding quantum defect functions is given in Fig. 2. Where possible, both the $n=2$ and $n=3$ quantum defects are given.

The above quantum defects for the $2s$ ($A\ 2\Sigma^+$), $2p$ ($C\ 2\Sigma$, $B\ 2\Pi$) and $3d$ ($D\ 2\Sigma^+$, $E\ 2\Pi$ and $1\ 2\Delta$) Rydberg states have been employed for the calculation of the electronic energies $E(R)$ for higher n Rydberg states and the resulting potentials are shown in Figs. 3 and 4, where for the

$2\Sigma^+$ states the $2s$ - $3s$ energy dependence and for the 2Π the $2p$ - $3p$ energy dependence has been incorporated in the quantum defects in a linear manner. Where available, the *ab initio* energies have been included as solid circles on the plots, for comparison. The good agreement between the *ab initio* data and the potentials obtained from the quantum defects is encouraging, in view of the single-channel approach adopted in the present work.

In order to aid in the assignment of Rydberg spectra of NeH and NeD vibrational levels of the Rydberg states have been calculated with the aid of the above quantum defect functions [cf. Eq. (19) and Table II] and in Table III, the $\nu=0$ level of several Rydberg states with principal quantum number n up to 10 have been given. For the $n=2$, s and p and the $n=3$, d states the $\nu=0$ levels calculated from the *ab initio* potentials directly are also given in brackets. As shown, there exist only slight differences between the *ab initio* levels and those obtained from the above expansion for the quantum defects. Further vibrational levels for Rydberg states of NeH (or NeD) may be produced with the aid of Eq. (6) and the present quantum defect functions, should a need for such data arise.

C. Complex scaling calculations

The results of the multi-state vibrational calculations on the $X\ 2\Sigma^+$, $A\ 2\Sigma^+$, $B\ 2\Pi$, and $C\ 2\Sigma^+$ states are summa-

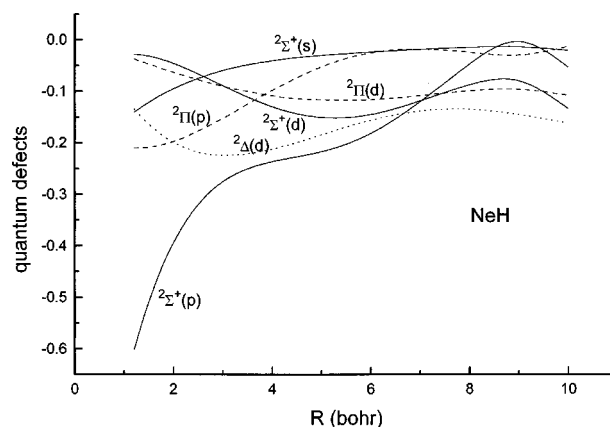


FIG. 2. Quantum defect functions for s , p , and d , $2\Sigma^+$ (solid lines), p and $d\ 2\Pi$ (dashed lines) and $d\ 2\Delta$ (dotted lines) Rydberg states of NeH.

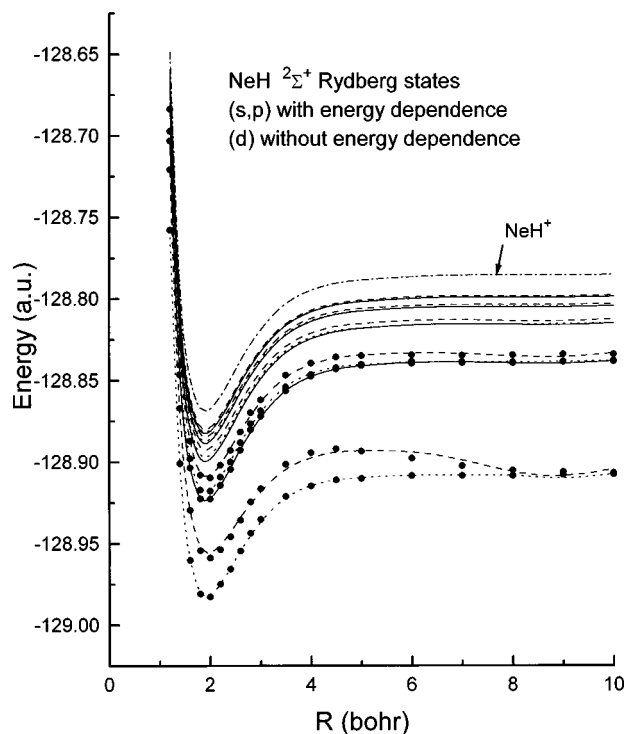


FIG. 3. Potential energy curves for s (dotted lines), p (dashed lines), and d (solid lines) $^2\Sigma^+$ Rydberg states of NeH generated with the aid of the quantum defect functions. Solid circles stand for *ab initio* data.

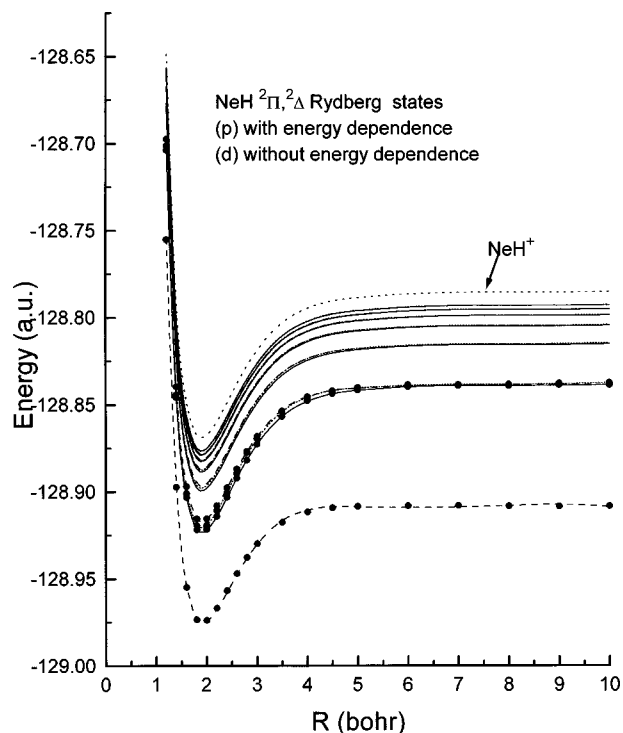


FIG. 4. Potential energy curves for p (dashed lines) and d (solid lines) $^2\Pi$ and d (dotted lines) $^2\Delta$ Rydberg states of NeH generated with the aid of the quantum defect functions. Solid circles stand for *ab initio* data.

TABLE III. Energies (hartree)^a of the $v=0$ levels of Rydberg states of NeH and NeD, obtained from the quantum defects.

n	$^2\Sigma^+(s)$	$^2\Sigma^+(p)$	$^2\Sigma^+(d)$	$^2\Pi(p)$	$^2\Pi(d)$	$^2\Delta(d)$
NeH						
2	-0.97688 (-0.97699) ^b	-0.95293 (-0.95290) ^c	-----	-0.96868 (-0.96873) ^d	-----	-----
3	-0.91394	-0.90617	-0.91745 (-0.91750) ^e	-0.91137	-0.91660 (-0.91665) ^f	-0.91401 (-0.91407) ^g
4	-0.89126	-0.88781	-0.89275	-0.89014	-0.89239	-0.89128
5	-0.88059	-0.87877	-0.88135	-0.88001	-0.88117	-0.88060
6	-0.87473	-0.87366	-0.87518	-0.87439	-0.87507	-0.87474
7	-0.87118	-0.87050	-0.87146	-0.87097	-0.87140	-0.87119
8	-0.86887	-0.86840	-0.86905	-0.86872	-0.86901	-0.86887
9	-0.86727	-0.86694	-0.86740	-0.86717	-0.86737	-0.86727
10	-0.86613	-0.86589	-0.86622	-0.86605	-0.86620	-0.86613
NeD						
2	-0.97867 (-0.97874)	-0.95451 (-0.95450)	-----	-0.97042 (-0.97043)	-----	-----
3	-0.91573	-0.90788	-0.91929 (-0.91930)	-0.91315	-0.91839 (-0.91840)	-0.91585 (-0.91587)
4	-0.89304	-0.88957	-0.89456	-0.89192	-0.89418	-0.89309
5	-0.88238	-0.88054	-0.88315	-0.88179	-0.88296	-0.88240
6	-0.87652	-0.87544	-0.87698	-0.87618	-0.87686	-0.87654
7	-0.87297	-0.87228	-0.87326	-0.87275	-0.87319	-0.87298
8	-0.87065	-0.87019	-0.87085	-0.87051	-0.87080	-0.87066
9	-0.86906	-0.86873	-0.86919	-0.86896	-0.86916	-0.86906
10	-0.86792	-0.86767	-0.86801	-0.86784	-0.86799	-0.86792

^aEnergy given with respect to -128.000000 hartree. *Ab initio* values in brackets.

^bA $^2\Sigma^+$.

^cC $^2\Sigma^+$.

^dB $^2\Pi$.

^eD $^2\Sigma^+$.

^fE $^2\Pi$.

^gI $^2\Delta$.

TABLE IV. Energies half-widths and predissociation lifetimes of vibrational levels of the $A\ ^2\Sigma^+$, $C\ ^2\Sigma^+$, and $B\ ^2\Pi$ states of NeH.

	Energy ^a (cm ⁻¹)	$c^2(A\ ^2\Sigma^+)$	$c^2(C\ ^2\Sigma^+)$	$c^2(B\ ^2\Pi)$	$\Gamma/2$ (hartree)	Lifetime (s)
<i>N</i> = 1						
$A\ ^2\Sigma^+ v=0$	0	0.9972	0.0027	0.0001	0.65E-08	0.19E-08
$B\ ^2\Pi v=0$	1819	0.0002	0.0000	0.9998	0.90E-12	0.13E-04
$A\ ^2\Sigma^+ v=1$	2543	0.9733	0.0265	0.0002	0.14E-07	0.83E-09
$B\ ^2\Pi v=1$	4370	0.0004	0.0001	0.9995	0.60E-11	0.20E-05
$A\ ^2\Sigma^+ v=2$	4780	0.8997	0.0998	0.0004	0.19E-07	0.63E-09
$C\ ^2\Sigma^+ v=0$	5404	0.0854	0.9145	0.0001	0.43E-09	0.28E-07
$B\ ^2\Pi v=2$	6685	0.0009	0.0001	0.9990	0.17E-10	0.68E-06
$A\ ^2\Sigma^+ v=3$	6973	0.9316	0.0673	0.0010	0.20E-07	0.62E-09
$C\ ^2\Sigma^+ v=1$	7837	0.0551	0.9448	0.0001	0.60E-10	0.20E-06
$B\ ^2\Pi v=3$	8733	0.0016	0.0001	0.9983	0.24E-10	0.50E-06
$A\ ^2\Sigma^+ v=4$	8930	0.9348	0.0634	0.0017	0.13E-07	0.88E-09
$C\ ^2\Sigma^+ v=2$	10117	0.0706	0.9293	0.0001	0.11E-09	0.11E-06
$B\ ^2\Pi v=4$	10584	0.0243	0.0015	0.9742	0.21E-09	0.58E-07
$A\ ^2\Sigma^+ v=5$	10629	0.9111	0.0630	0.0257	0.74E-08	0.16E-08
$A\ ^2\Sigma^+ v=6$	12029	0.8975	0.1016	0.0008	0.19E-08	0.64E-08
$B\ ^2\Pi v=5$	12172	0.0004	0.0027	0.9969	0.31E-11	0.39E-05
$C\ ^2\Sigma^+ v=3$	12283	0.1147	0.8830	0.0022	0.23E-08	0.52E-08
<i>N</i> = 10						
$A\ ^2\Sigma^+ v=0$	1753	0.9950	0.0027	0.0023	0.54E-08	0.22E-08
$B\ ^2\Pi v=0$	3596	0.0096	0.0023	0.9881	0.43E-10	0.28E-06
$A\ ^2\Sigma^+ v=1$	4057	0.9691	0.0209	0.0099	0.12E-07	0.10E-08
$B\ ^2\Pi v=1$	6019	0.0306	0.0040	0.9654	0.37E-09	0.33E-07
$A\ ^2\Sigma^+ v=2$	6358	0.8924	0.0764	0.0312	0.16E-07	0.76E-09
$C\ ^2\Sigma^+ v=0$	7047	0.0626	0.9342	0.0032	0.22E-09	0.55E-07
$B\ ^2\Pi v=2$	8207	0.0567	0.0059	0.9374	0.91E-09	0.13E-07
$A\ ^2\Sigma^+ v=3$	8465	0.8796	0.0605	0.0599	0.16E-07	0.74E-09
$C\ ^2\Sigma^+ v=1$	9380	0.0543	0.9425	0.0032	0.16E-09	0.77E-07
$B\ ^2\Pi v=3$	10141	0.1372	0.0098	0.8529	0.19E-08	0.63E-08
$A\ ^2\Sigma^+ v=4$	10298	0.8042	0.0510	0.1447	0.12E-07	0.10E-08
$C\ ^2\Sigma^+ v=2$	11568	0.1183	0.8781	0.0035	0.56E-12	0.22E-04
$A\ ^2\Sigma^+ v=5$	11808	0.6374	0.0717	0.2909	0.70E-08	0.17E-08
$B\ ^2\Pi v=4$	11917	0.2520	0.0422	0.7058	0.26E-08	0.46E-08
$A\ ^2\Sigma^+ v=6$	13084	0.9307	0.0513	0.0178	0.45E-08	0.27E-08
$B\ ^2\Pi v=5$	13318	0.0146	0.0131	0.9723	0.35E-11	0.34E-05
$C\ ^2\Sigma^+ v=3$	13644	0.0754	0.9152	0.0094	0.21E-08	0.59E-08

^aGiven with respect to -128.976942 hartree.

rized in Tables IV and V for NeH and NeD, respectively, in terms of energies, the squares of coefficients for the above three excited states, half-widths and the corresponding predissociation lifetimes of the resonances for rotational levels $N=1$ and $N=10$. As shown in Tables IV and V, there is some mixing of the levels of the $A\ ^2\Sigma^+$ and $C\ ^2\Sigma^+$ states and there is also interaction with the levels of the $B\ ^2\Pi$ state for high rotational levels (cf. results for $N=10$). Predissociation is significant in NeH, especially for the levels of the $A\ ^2\Sigma^+$ state, where it is faster than radiative dissociation¹⁴ by a factor of 15 for $v=0$ and about 50 for higher vibrational levels. Similarly, predissociation is important for the levels of the $C\ ^2\Sigma^+$ in NeH, with lifetimes slightly longer than radiative dissociation (e.g. by a factor of 4 for $v=0$). Predissociation is not significant for the levels of the $B\ ^2\Pi$ state in NeH for $N=1$ while for $N=10$ it gains some importance and for $v \geq 1$ levels (of the $B\ ^2\Pi^+$ component) it becomes comparable to radiative dissociation.¹⁴

The calculated widths in NeD (cf. Table V) are generally

smaller than those in NeH. In particular for the levels of the $A\ ^2\Sigma^+$ state there is strong suppression of predissociation in NeD compared to NeH, in agreement with previous calculations and experimental findings, with a ratio $\Gamma_{\text{NeH}}/\Gamma_{\text{NeD}} = 177$ for $v=0$ ($N=1$). This is comparable to the Fermi Golden Rule ratio of 120 and the overlap ratio of 140 for $v=0$, $N=0$.¹⁷ Such a strong isotope effect is not found for the levels of the $C\ ^2\Sigma^+$ state, except for the $v=3$ $N=1$ level, while for the $B\ ^2\Pi$ state a strong isotope effect is found for vibrational levels higher than $v=2$. As illustrated elsewhere,¹⁷ such isotope effects in the rare gas hydrides may be attributed to differences in the overlap and d/dR integrals over the vibrational wavefunctions. Thus in NeD radiative transitions are more probable than predissociation and even in NeH where predissociation is more significant, the predissociation rates are not such that would preclude the observation of radiative transitions.

The present calculations do not support the formation of “ $p(\Sigma, \Pi)$ ” complex in NeH and in NeD since even for N

TABLE V. Energies half-widths and predissociation lifetimes of vibrational levels of the $A\ ^2\Sigma^+$, $C\ ^2\Sigma^+$, and $B\ ^2\Pi$ states of NeD.

	Energy ^a (cm ⁻¹)	$c^2(A\ ^2\Sigma^+)$	$c^2(C\ ^2\Sigma^+)$	$c^2(B\ ^2\Pi)$	$\Gamma/2$ (hartree)	Lifetime (s)
<i>N</i> = 1						
$A\ ^2\Sigma^+ v=0$	0	0.9987	0.0013	0.0000	0.37E-10	0.33E-06
$B\ ^2\Pi v=0$	1826	0.0007	0.0000	0.9992	0.60E-13	0.20E-03
$A\ ^2\Sigma^+ v=1$	1947	0.9904	0.0088	0.0008	0.12E-09	0.10E-06
$A\ ^2\Sigma^+ v=2$	3685	0.9765	0.0146	0.0088	0.21E-09	0.57E-07
$B\ ^2\Pi v=1$	3727	0.0087	0.0001	0.9912	0.24E-11	0.51E-05
$A\ ^2\Sigma^+ v=3$	5315	0.5764	0.4233	0.0002	0.20E-09	0.61E-07
$C\ ^2\Sigma^+ v=0$	5379	0.4133	0.5860	0.0007	0.17E-09	0.73E-07
$B\ ^2\Pi v=3$	5507	0.0009	0.0001	0.9990	0.73E-12	0.16E-04
$A\ ^2\Sigma^+ v=4$	6932	0.9587	0.0408	0.0005	0.52E-09	0.23E-07
$B\ ^2\Pi v=4$	7133	0.0002	0.0023	0.9974	0.85E-12	0.14E-04
$C\ ^2\Sigma^+ v=1$	7163	0.0322	0.9657	0.0021	0.23E-10	0.53E-06
$A\ ^2\Sigma^+ v=5$	8428	0.9767	0.0228	0.0004	0.72E-09	0.17E-07
$B\ ^2\Pi v=5$	8633	0.0004	0.0001	0.9995	0.64E-12	0.19E-04
$C\ ^2\Sigma^+ v=2$	8849	0.0176	0.9824	0.0000	0.28E-10	0.43E-06
$A\ ^2\Sigma^+ v=6$	9783	0.9780	0.0217	0.0002	0.83E-09	0.15E-07
$B\ ^2\Pi v=6$	10036	0.0002	0.0000	0.9997	0.15E-11	0.82E-05
$C\ ^2\Sigma^+ v=3$	10483	0.0199	0.9801	0.0000	0.49E-10	0.24E-06
<i>N</i> = 10						
$A\ ^2\Sigma^+ v=0$	936	0.9980	0.0013	0.0007	0.30E-10	0.40E-06
$B\ ^2\Pi v=0$	2770	0.1059	0.0021	0.8921	0.72E-11	0.17E-05
$A\ ^2\Sigma^+ v=1$	2846	0.8861	0.0064	0.1074	0.88E-10	0.14E-06
$A\ ^2\Sigma^+ v=2$	4528	0.9133	0.0137	0.0730	0.14E-09	0.86E-07
$B\ ^2\Pi v=1$	4637	0.0726	0.0010	0.9264	0.19E-10	0.63E-06
$A\ ^2\Sigma^+ v=3$	6146	0.8213	0.1631	0.0155	0.19E-09	0.65E-07
$C\ ^2\Sigma^+ v=0$	6256	0.1397	0.8385	0.0217	0.40E-10	0.30E-06
$B\ ^2\Pi v=2$	6375	0.0292	0.0081	0.9626	0.19E-10	0.65E-06
$A\ ^2\Sigma^+ v=4$	7718	0.9465	0.0352	0.0183	0.30E-09	0.40E-07
$C\ ^2\Sigma^+ v=1$	7950	0.0119	0.0406	0.9475	0.15E-10	0.82E-06
$C\ ^2\Sigma^+ v=2$	8002	0.0330	0.9327	0.0343	0.18E-10	0.66E-06
$A\ ^2\Sigma^+ v=5$	9170	0.9618	0.0223	0.0159	0.40E-09	0.30E-07
$B\ ^2\Pi v=3$	9411	0.0154	0.0027	0.9819	0.25E-10	0.48E-06
$C\ ^2\Sigma^+ v=3$	9655	0.0178	0.9800	0.0022	0.27E-10	0.45E-06
$A\ ^2\Sigma^+ v=6$	10472	0.9705	0.0207	0.0088	0.47E-09	0.26E-07
$B\ ^2\Pi v=4$	10768	0.0088	0.0012	0.9900	0.23E-10	0.54E-06
$C\ ^2\Sigma^+ v=4$	11266	0.0193	0.9796	0.0011	0.46E-10	0.26E-06

^aGiven with respect to -128.978706 hartree.

=10 the $B\ ^2\Pi$ state does not mix very heavily with the $A\ ^2\Sigma^+$ and $C\ ^2\Sigma^+$ states. Similar results as for $N=10$ have been obtained for $N=20$. However for the ($3d$) $D\ ^2\Sigma$, $E\ ^2\Pi$ and $1\ ^2\Delta$ states, the situation is different. A multi-state calculation of the vibrational levels of the $3d$ states, $D\ ^2\Sigma^+$, $E\ ^2\Pi$, and $1\ ^2\Delta$ (where only the positive parity components $^2\Pi^+$ and $^2\Delta^+$ are considered), including the rotational-electronic coupling has been carried out by a similar procedure as the above calculations but without any complex scaling (i.e. $\theta=0^\circ$). In Table VI the lowest two vibrational levels of the above states for different rotational quantum numbers N have been listed along with their mixing coefficients for both NeH and NeD. As shown, there is appreciable mixing between the $D\ ^2\Sigma^+$ and the $E\ ^2\Pi$ states and mixing to a smaller extent with the $1\ ^2\Delta$ state, at high rotational quantum numbers (cf. results for $N=10,20$). Thus, the present calculations predict the formation of a ($3d$) complex of states in NeH and in NeD. However, since such calculations are very sensitive to the energy difference between the

levels of the interacting states, the latter conclusions might be altered if the actual relative energies of the Rydberg states are far from the present theoretical predictions.

IV. CONCLUSION

In the present work, a theoretical study of the Rydberg states of NeH has been presented in an effort to aid future experimental work on the Rydberg spectra of this system. *Ab initio* calculations supplemented by quantum defect calculations have been employed for the generation of quantum defect functions, potential energy curves and vibrational levels of s , p , and d Rydberg states of NeH and NeD. Complex coordinate scaling calculations have been employed for the determination of the widths of the $2s$ and $2p$, $A\ ^2\Sigma^+$ and $C\ ^2\Sigma^+$, and $2p\ B\ ^2\Pi$ Rydberg states. The resulting predissociation lifetimes are roughly of the same order as the radiative lifetimes in NeH, while in NeD they are longer than

TABLE VI. Vibrational levels and coefficients of the $3d(^2\Sigma^+, ^2\Pi, ^2\Delta)$ states for different rotational levels N , in NeH and in NeD.

N	Energy ^a (cm ⁻¹)	$c^2(D\ ^2\Sigma^+)$	$c^2(E\ ^2\Pi)$	$c^2(1\ ^2\Delta)$	
NeH					
$N=2$	($v=0, D\ ^2\Sigma^+$)	13106	0.8321	0.1665	0.0013
	($v=0, E\ ^2\Pi$)	13350	0.1676	0.8183	0.0140
	($v=0, 1\ ^2\Delta$)	13874	0.0002	0.0151	0.9846
	($v=1, D\ ^2\Sigma^+$)	15790	0.7678	0.2306	0.0016
	($v=1, E\ ^2\Pi$)	15990	0.2321	0.7584	0.0095
($v=1, 1\ ^2\Delta$)	16560	0.0001	0.0110	0.9889	
$N=10$		14529	0.5170	0.4389	0.0441
		15205	0.4438	0.3255	0.2307
		15799	0.0392	0.2364	0.7244
		17110	0.5007	0.4580	0.0413
		17747	0.4698	0.3433	0.1869
	18331	0.0302	0.1986	0.7712	
$N=20$		19015	0.4259	0.4892	0.0849
		20102	0.4747	0.1486	0.3767
		20961	0.0970	0.3746	0.5283
		21278	0.4435	0.4695	0.0869
		22290	0.4703	0.1668	0.3628
	23095	0.0871	0.3668	0.5461	
NeD					
$N=2$		13080	0.9436	0.0562	0.0001
		13291	0.0564	0.9395	0.0042
		13830	0.0000	0.0043	0.9957
		15108	0.8919	0.1078	0.0002
		15256	0.1081	0.8890	0.0029
	15853	0.0000	0.0031	0.9968	
$N=10$		13874	0.6645	0.3216	0.0139
		14288	0.3294	0.5820	0.0886
		14816	0.0062	0.0967	0.8971
		15847	0.5989	0.3861	0.0150
		16227	0.3970	0.5402	0.0629
	16783	0.0043	0.0741	0.9216	
$N=20$		16345	0.5281	0.4294	0.0425
		17021	0.4356	0.3390	0.2254
		17628	0.0359	0.2346	0.7294
		18183	0.5067	0.4510	0.0424
		18826	0.4662	0.3484	0.1854
	19427	0.0285	0.2007	0.7708	

^aWith respect to -128.976942 hartree for NeH (cf. Table IV) and -128.978706 hartree for NeD (cf. Table V).

the radiative lifetimes. Finally, a calculation of the interaction between the $3d\ D\ ^2\Sigma^+$, $E\ ^2\Pi^+$ and $1\ ^2\Delta^+$ states, shows strong mixing of the vibrational states for high values of the rotational quantum number (i.e., $N \geq 10$).

ACKNOWLEDGMENT

I.D.P. is an Alexander von Humboldt-Fellow 1996–1997.

- ¹G. Herzberg, *Annu. Rev. Phys. Chem.* **38**, 27 (1987).
- ²G. Theodorakopoulos, S. C. Farantos, R. J. Buenker, and S. D. Peyerimhoff, *J. Phys. B* **17**, 1453 (1984).
- ³J. W. C. Johns, *J. Mol. Spectrosc.* **36**, 488 (1970).
- ⁴W. Ketterle, H. Figger, and H. Walther, *Phys. Rev. Lett.* **55**, 2941 (1985).
- ⁵W. Ketterle, *J. Chem. Phys.* **93**, 6935 (1990); **93**, 6929 (1990); **93**, 3760 (1990); **93**, 3752 (1990).
- ⁶I. Dabrowski, D. W. Tokaryk, M. Vervloet, and J. K. G. Watson, *J. Chem. Phys.* **104**, 8245 (1996); I. Dabrowski and D. A. Sadovskii, *Mol. Phys.* **81**, 291 (1994); M. Douay, S. A. Rogers, and P. F. Bernath, *ibid.* **64**, 425 (1988); I. Dabrowski, G. Herzberg, and R. H. Lipson, *ibid.* **63**, 289 (1988).
- ⁷T. Möller, M. Beland, and G. Zimmerer, *Chem. Phys. Lett.* **136**, 551 (1987).
- ⁸P. Devynck, W. G. Graham, and J. R. Peterson, *J. Chem. Phys.* **91**, 6880 (1989).
- ⁹G. I. Gellene, *J. Chem. Phys.* **93**, 2960 (1990).
- ¹⁰B. Stenum, J. Schou, and P. Gürtler, *Chem. Phys. Lett.* **229**, 353 (1994).
- ¹¹W. Ketterle, dissertation, Universität München, 1986.
- ¹²W. Ketterle and H. Walther, *Chem. Phys. Lett.* **146**, 180 (1988).
- ¹³G. Theodorakopoulos, I. D. Petsalakis, and R. J. Buenker, *J. Phys. B* **20**, 5335 (1987).
- ¹⁴I. D. Petsalakis, G. Theodorakopoulos, and R. J. Buenker, *Phys. Rev. A* **38**, 4004 (1988).
- ¹⁵I. D. Petsalakis, Th. Mercouris, G. Theodorakopoulos, and C. A. Nicolaides, *J. Chem. Phys.* **93**, 6642 (1990).
- ¹⁶I. D. Petsalakis, Th. Mercouris, and C. A. Nicolaides, *Chem. Phys.* **189**, 615 (1994).
- ¹⁷I. D. Petsalakis and G. Theodorakopoulos, *J. Phys. B* **25**, 5353 (1992).
- ¹⁸Y. Li, O. Bludský, G. Hirsch, and R. J. Buenker, *J. Chem. Phys.* (in press).
- ¹⁹I. D. Petsalakis, G. Theodorakopoulos, G. Hirsch, and R. J. Buenker, *J. Phys. B* (in press).
- ²⁰I. Dabrowski, G. Dilonardo, G. Herzberg, J. W. C. Johns, D. A. Sadovskii, and M. Vervloet, *J. Chem. Phys.* **97**, 7093 (1992).
- ²¹G. Theodorakopoulos, I. D. Petsalakis, and R. J. Buenker, *Mol. Phys.* **71**, 1055 (1990); G. Theodorakopoulos and I. D. Petsalakis, *J. Chem. Phys.* **101**, 194 (1994).
- ²²R. J. Buenker, in *Studies in Physical and Theoretical Chemistry, Current Aspects of Quantum Chemistry 1981*, edited by R. Carbo (Elsevier, Amsterdam, 1982), Vol. 2, p. 17; R. J. Buenker and R. A. Phillips, *J. Mol. Struct.: THEOCHEM* **123**, 291 (1985).
- ²³S. Huzinaga, *J. Chem. Phys.* **42**, 1293 (1965).
- ²⁴T. H. Dunning, Jr., *J. Chem. Phys.* **55**, 716 (1971).
- ²⁵I. D. Petsalakis, G. Theodorakopoulos, and V. J. Barclay, *Chem. Phys. Lett.* **160**, 189 (1989).
- ²⁶S. R. Langhoff and E. R. Davidson, *Int. J. Quantum Chem.* **8**, 61 (1974).
- ²⁷M. Seaton, *Rep. Prog. Phys.* **46**, 167 (1983).
- ²⁸C. H. Greene and Ch. Jungen, *Adv. At. Mol. Phys.* **21**, 51 (1985).
- ²⁹S. C. Ross and Ch. Jungen, *Phys. Rev. A* **49**, 4353 (1994); **49**, 4364 (1994).
- ³⁰I. D. Petsalakis, G. Theodorakopoulos, and M. S. Child, *J. Phys. B* **28**, 5179 (1995).
- ³¹G. Theodorakopoulos, I. D. Petsalakis, and M. S. Child, *J. Phys. B* **29**, 4543 (1996).
- ³²S. Fredin, D. Gauyacq, M. Horani, Ch. Jungen, G. Lefevre, and F. Masnou-Seeuws, *Mol. Phys.* **60**, 825 (1987).
- ³³Ch. Jungen, A. L. Roche, and M. Arif, *Philos. Trans. R. Soc. London, Ser. A* **355**, 1481 (1997).
- ³⁴O. Atabek and R. Lefebvre, *Phys. Rev. A* **22**, 1817 (1980).
- ³⁵N. Moiseyev, *Int. J. Quantum Chem.* **20**, 835 (1981).
- ³⁶J. Turner and C. W. McCurdy, *Chem. Phys.* **71**, 127 (1982).
- ³⁷Th. Mercouris and C. A. Nicolaides, *Z. Phys. D* **5**, 1 (1987).
- ³⁸P. Pendergast, J. M. Heck, and E. F. Hays, *Int. J. Quantum Chem.* **49**, 495 (1994).